RESEARCH ARTICLE

The properties of MOF-Zn$_2$(EBNB)$_2$(BPY)$_2$·2H$_2$O and its basic study of loading methadone

Deng Linxin[1†], Li Song[2†] and Sun Xuehua[1*]

Abstract

The ligands of (E)-bis(p-3-nitrobenzoic acid) vinyl (C$_{16}$H$_{10}$N$_2$O$_8$) were synthesized in three steps, and then the MOF-Zn$_2$(EBNB)$_2$(BPY)$_2$·2H$_2$O was synthesized by solvothermal method. This structure was characterized by X-ray single crystal diffraction, SEM and TG. The drug loading and in vitro release of Zn$_2$(EBNB)$_2$(BPY)$_2$·2H$_2$O were also studied with Methadone as model drug. The results show that the highest loading amount of Zn$_2$(EBNB)$_2$(BPY)$_2$·2H$_2$O to Methadone was 0.256 g/g, and the drug delivery system was a two-phase mode. The results of in vitro cytotoxicity test show that Zn$_2$(EBNB)$_2$(BPY)$_2$·2H$_2$O has good biocompatibility.

Keywords: MOFs, Methadone, Drug loading, Drug release, Cytotoxicity

Introduction

Methadone is the main drug in current opioid drugs addiction replacement therapy [1]. Methadone can bind to opioid receptors competitively in human body, and can produce cross dependence and tolerance with opioids such as heroin, thus it can reduce the sensitivity of opioid receptors in drug dependent patients [2]. At the same time, combined with psychotherapy, behavioral intervention and other comprehensive measures, methadone can eventually reduce the harm of drugs and the demand for drugs to addicts [3].

The dosage of methadone has been a controversial issue. There are many studies supporting the use of high-dose methadone, that is to say, the higher the dosage of methadone, the longer the holding time of patients, and the better effect of alternative maintenance therapy [4]. However, methadone itself is addictive, and long-term or high-dose use is easy to lead to addiction [5]. Nevertheless, the action time of low-dose methadone (such as 2.5–5 mg) is only 6-8 h [6], which is not convenient for clinical use.

At present, the research hotspots of methadone replacement maintenance therapy focus mainly on the cognitive survey of patients with methadone maintenance treatment [7], the operation of methadone outpatient service [8], the retention rate and its influencing factors in methadone maintenance treatment [9], and the cost-effectiveness of methadone maintenance treatment [10].

As one of the advanced frontier materials, metal organic frameworks(MOFs) is the fastest developing direction of coordination chemistry in recent 10 years [11]. It has a super molecular network structure [12], and has the advantages of both inorganic and organic compounds [13]. The structure of this kind of frame material can realize diversified design and adjustable pore size or structure. So it can realize semi directional design synthesis [14]. The research of this kind of molecular functional materials has spanned many fields such as crystallography, materials science, inorganic chemistry, coordination chemistry, organic chemistry, etc. [15]. As a new type of nano porous material, comparing with activated carbon and zeolite, MOFs have been widely used in the fields of gas capture, storage and separation [16]; drug release [17]; optical, magnetic, electrical science [18]; catalytic science [19]; chiral resolution [20] and so on.

*Correspondence: sirleee@live.cn
†Deng Linxin and Li Song contributed equally to this work
[1] Department of Drug Control, Key Laboratory of Narcotics Assay and Control Technology Ministry of Public Security, Yunnan Police College, Kunming 650223, China
Full list of author information is available at the end of the article

Linxin *et al. BMC Chemistry*   (2020) 14:57

Page 2 of 8

$Zn_2(EBNB)_2(BPY)_2 \cdot 2H_2O$ is a new type of 3D porous MOFs material [21]. It has excellent gas adsorption performance in study of many kinds of gas molecules, but it has not been reported as a drug carrier. In this paper, we use methadone as the model drug, and optimized the preparation process of the drug carrier by two factors. We investigated the in vitro release characteristics and in vitro cytotoxicity experiment of the drug carrier $Zn_2(EBNB)_2(BPY)_2 \cdot 2H_2O$, which provided the foundation for its development and application as a drug carrier.

Results and discussion

Chemistry

The synthesis of $Zn_2(EBNB)_2(BPY)_2 \cdot 2H_2O$ by solvothermal method began with the synthesis of (E)—bis (p-3-nitrobenzoic acid) ethylene ligand ($C_{16}H_{10}N_2O_8$) which was synthesized by Nitrification and coupling from p-chloromethylbenzoic acid (Scheme 1).

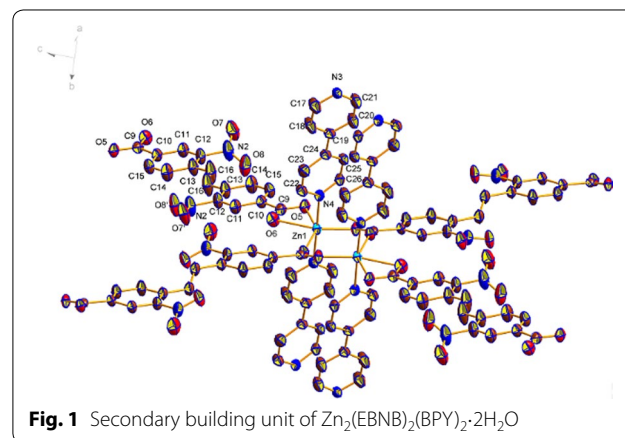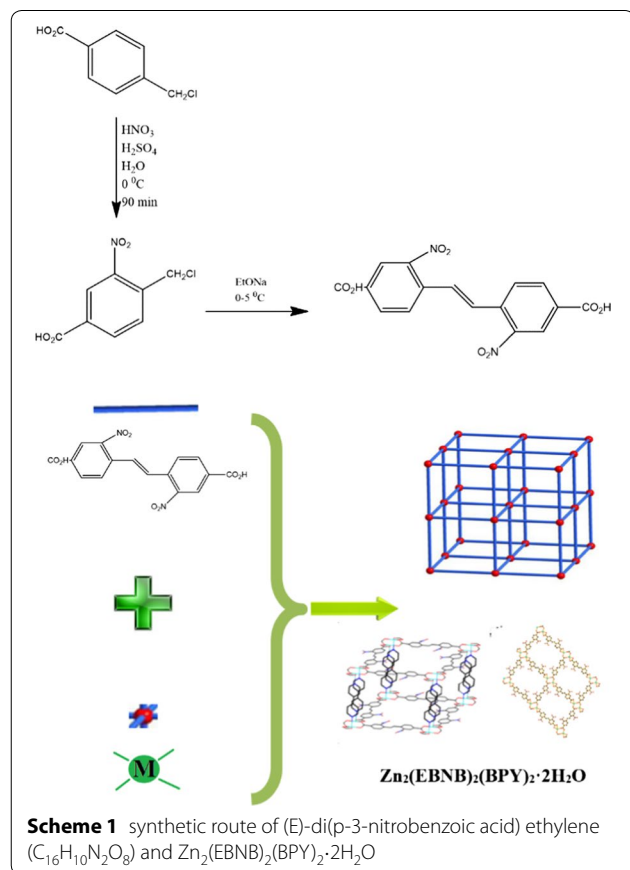### Crystal structures of $Zn_2(EBNB)_2(BPY)_2 \cdot 2H_2O$

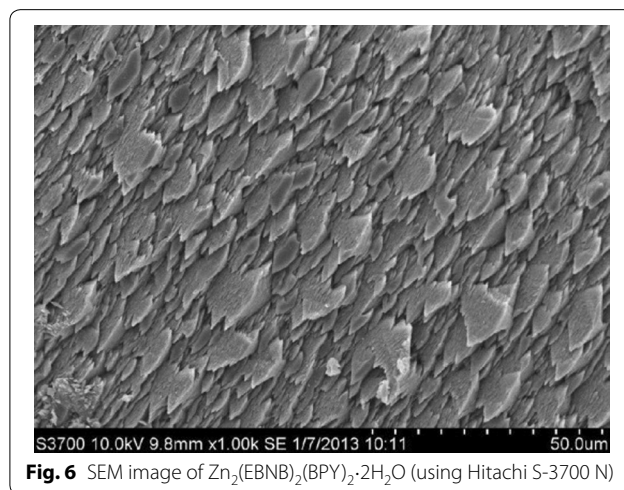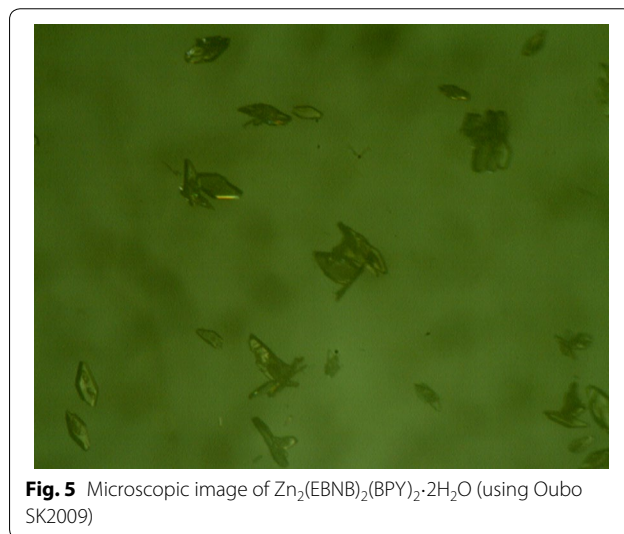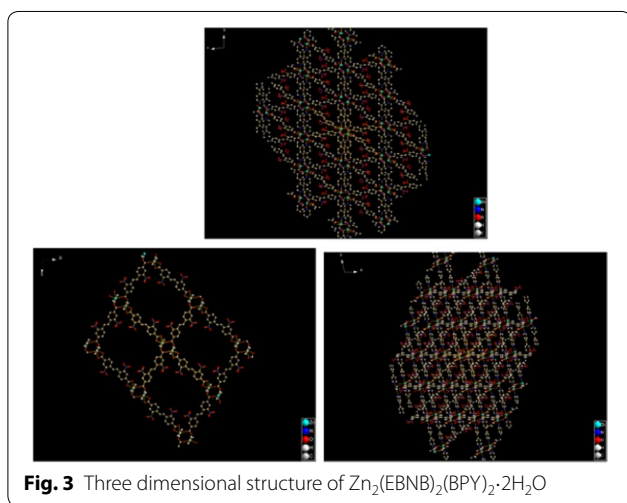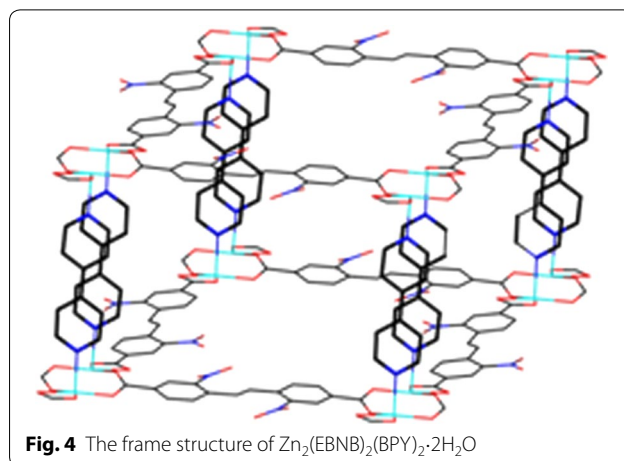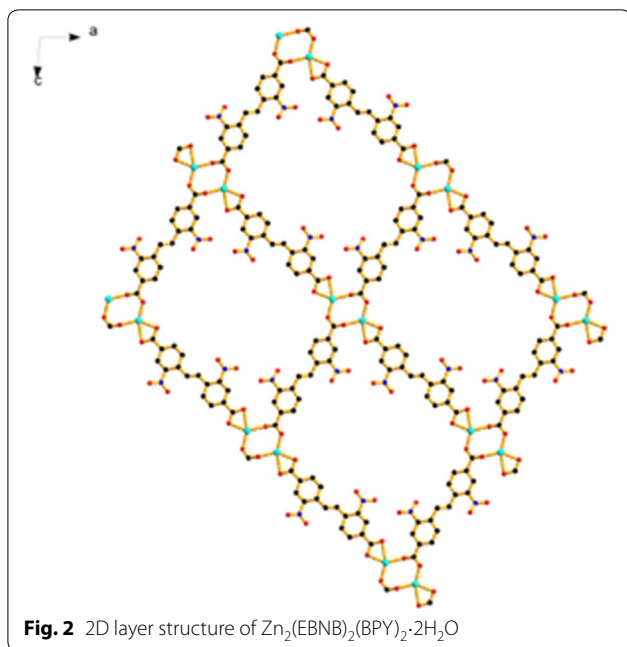Single X-ray crystal diffraction analysis reveals that compound 1 crystallizes in the P-1 space group, and possesses an extended 3D framework with a novel dinuclear Zinc clusters as secondly build unit. In dinuclear Zinc unit, each Zn^{2+} is connected by four oxygen atoms, two of which come from the same EBNB ligand, as shown in Fig. 1. The distance of Zn–O is 2.03 Å. The remaining two oxygen atoms come from two different EBNB ligand respectively (Fig. 1), and the distance of Zn–O is 2.13 and 2.17 Å respectively. The EBNB also have two coordination modes with the Zn^{2+}, first one is the carboxylic oxygen atom links to one Zn^{2+}, and the other is two oxygen atoms connect to two Zn^{2+} respectively. Each cluster unit is linked with neighboring units through four EBNB ligands to form a 2D layer (Fig. 2). Four BPY molecules serve as pillar ligands to coordinate with the outer Zn atoms which gives raise to 3D framework (Fig. 3).

Figure 1 also shows that a single (E)-di(p-3-nitrobenzoic acid) ethylene ligand is coordinated with two Zn (II) ions along the AC plane, and each Zn (II) ion is also coordinated with an oxygen coordination atom in a water molecule and two (E)-di(p-3-nitrobenzoic acid) ethylene ligands, thus extending outward to form a 2D plane. Along the c-axis direction, the layers and the interlayer are connected with Zn (II) ion via bipyridine column ligand to build a 3D network structure. And finally, a 3D metal organic framework material with one-dimensional pore structure is formed (Figs. 2, 3 and 4).

Microscope and SEM image of $Zn_2(EBNB)_2(BPY)_2 \cdot 2H_2O$

The morphology of $Zn_2(EBNB)_2(BPY)_2 \cdot 2H_2O$ was characterized by microscope and SEM. Figure 5 is a microscope picture of $Zn_2(EBNB)_2(BPY)_2 \cdot 2H_2O$. It can be seen from Fig. 5 that it is yellow diamond crystal. Figure 6 shows the surface morphology of $Zn_2(EBNB)_2(BPY)_2 \cdot 2H_2O$ in SEM. It can be seen from Fig. 6 that the surface structure of $Zn_2(EBNB)_2(BPY)_2 \cdot 2H_2O$ is fish scale.

Scheme 1 synthetic route of (E)-di(p-3-nitrobenzoic acid) ethylene ($C_{16}H_{10}N_2O_8$) and $Zn_2(EBNB)_2(BPY)_2 \cdot 2H_2O$

Fig. 1 Secondary building unit of $Zn_2(EBNB)_2(BPY)_2 \cdot 2H_2O$

Linxin *et al. BMC Chemistry* (2020) 14:57

Page 3 of 8

Fig. 2 2D layer structure of $Zn_2(EBNB)_2(BPY)_2 \cdot 2H_2O$

Fig. 3 Three dimensional structure of $Zn_2(EBNB)_2(BPY)_2 \cdot 2H_2O$

Fig. 4 The frame structure of $Zn_2(EBNB)_2(BPY)_2 \cdot 2H_2O$

Fig. 5 Microscopic image of $Zn_2(EBNB)_2(BPY)_2 \cdot 2H_2O$ (using Oubo SK2009)

Fig. 6 SEM image of $Zn_2(EBNB)_2(BPY)_2 \cdot 2H_2O$ (using Hitachi S-3700 N)

Powder XRD characterization of $Zn_2(EBNB)_2(BPY)_2 \cdot 2H_2O$

Figure 7 is the powder XRD characterization of $Zn_2(EBNB)_2(BPY)_2 \cdot 2H_2O$ which are actual measured, software simulation's and ligand's. Among it, A is the ligand bipyridine's XRD, B is the (E)-di(p-3-nitrobenzoic acid) ethylene ligand's XRD, C is the $Zn_2(EBNB)_2(BPY)_2 \cdot 2H_2O$'s actual measured XRD, and D is the $Zn_2(EBNB)_2(BPY)_2 \cdot 2H_2O$'s simulated XRD. It can be seen from the figure that the measured value of $Zn_2(EBNB)_2(BPY)_2 \cdot 2H_2O$ is in good agreement with the simulated value of the software, which shows that the
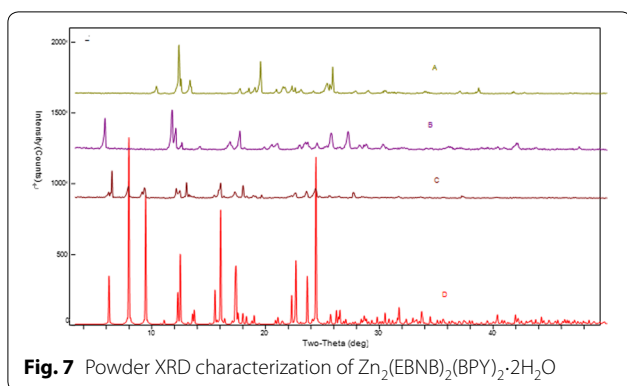
Linxin *et al. BMC Chemistry*   (2020) 14:57

Page 4 of 8

Fig. 7 Powder XRD characterization of $Zn_2(EBNB)_2(BPY)_2 \cdot 2H_2O$

compound is a pure phase, and there are obvious differences compare with the two ligands.

Thermal analysis of $Zn_2(EBNB)_2(BPY)_2 \cdot 2H_2O$

The thermal gravimetric analysis of $Zn_2(EBNB)_2 (BPY)_2 \cdot 2H_2O$ was carried out by DSC-TG in the temperature range of 0 °C to 600 °C. Figure 8 is the DSC-TG diagram of $Zn_2(EBNB)_2(BPY)_2 \cdot 2H_2O$. It can be seen from the figure that $Zn_2(EBNB)_2(BPY)_2 \cdot 2H_2O$ can be stabilized to 350 °C. $Zn_2(EBNB)_2(BPY)_2 \cdot 2H_2O$ lost 3.78% of its first thermal weight in the temperature range of 50–200 °C, which can be attributed to the loss of guest molecules. However, in the temperature range of 350 °C ~ 560 °C, the structure collapses, resulting in 46.58% weight loss. The main component is ZnO.

Study on sustained release of drug

Determination of drug loading of $Zn_2(EBNB)_2(BPY)_2 \cdot 2H_2O$

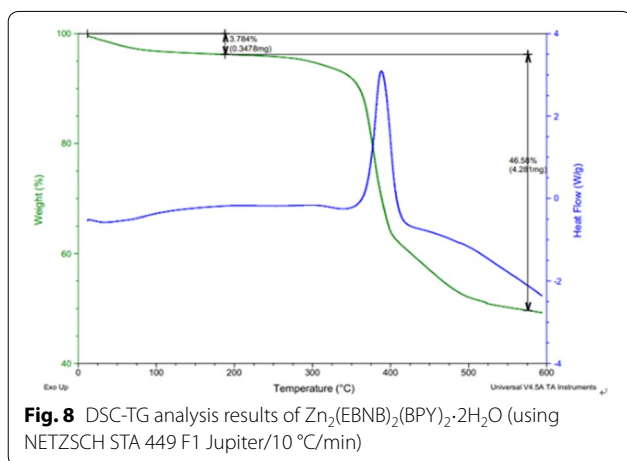The maximum absorption peak of Methadone methanol solution is 292 nm.

Fig. 8 DSC-TG analysis results of $Zn_2(EBNB)_2(BPY)_2 \cdot 2H_2O$ (using NETZSCH STA 449 F1 Jupiter/10 °C/min)

Table 1 shows the relationship between the ratio of Methadone to carrier mass and the drug loading time to the drug loading of $Zn_2(EBNB)_2(BPY)_2 \cdot 2H_2O$. It can be seen that with the increase of the ratio of Methadone to carrier mass (fixed carrier mass, increasing drug mass), the drug loading of $Zn_2(EBNB)_2(BPY)_2 \cdot 2H_2O$ increases. Also,the longer the action time, the higher the loading of $Zn_2(EBNB)_2(BPY)_2 \cdot 2H_2O$. However, the highest loading of $Zn_2(EBNB)_2(BPY)_2 \cdot 2H_2O$ appeared on the 5th day under different drug to carrier mass ratio. This explains that the drug loading amount of $Zn_2(EBNB)_2(BPY)_2 \cdot 2H_2O$ reaches the maximum value at the 5th day of adsorption.

However, when the action time is extended to 7 days, the drug loading amount will decrease, which may be caused by the falling off of some drugs adsorbed on the surface of $Zn_2(EBNB)_2(BPY)_2 \cdot 2H_2O$ due to the long immersion time. This indicates that the best action time is 5 days. It can be seen from Table 1 that the best experimental condition of the mass ratio of the drug to the carrier is 5:1, the best action time is 5 days, and the highest drug loading can be obtained is 0.256 g/g carrier.

In vitro release of Methadone loaded by $Zn_2(EBNB)_2(BPY)_2 \cdot 2H_2O$
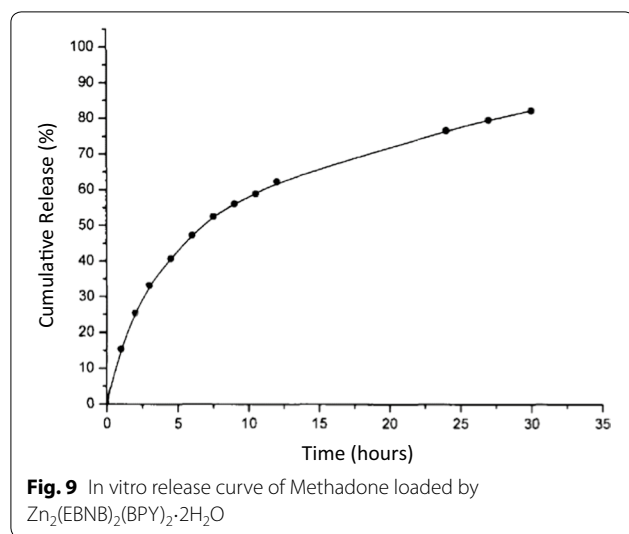
As shown in Fig. 9, the drug release process is divided into two processes. The first 5 h of the drug release curve shows the characteristics of sudden release, and the sudden release of Methadone is 40.1% within 5 h. This is mainly due to the diffusion of the Methadone which adsorbed on the surface of $Zn_2(EBNB)_2(BPY)_2 \cdot 2H_2O$ into the medium. And then it enters a stable and slow release stage, those Methadone adsorbed in the $Zn_2(EBNB)_2(BPY)_2 \cdot 2H_2O$ channel is being released slowly. Within 30 h of stable release, the release amount of Methadone reached 79.85%, showing a significant slow-release effect.

Cytotoxic test results of $Zn_2(EBNB)_2(BPY)_2 \cdot 2H_2O$

In this study, normal growth cells $(Zn_2(EBNB)_2 (BPY)_2 \cdot 2H_2O$'s concentration of 0 µg · ML^{-1}) were used as the negative control group, and $Zn_2(EBNB)_2(BPY)_2 \cdot 2H_2O$

Table 1 Loading amount of Methadone (m_2) on $Zn_2(EBNB)_2(BPY)_2 \cdot 2H_2O$ (m_1) (n = 3)

$M2/m1$	Drug loading ratio m2/m1			
	1 day	**3 day**	**5 day**	**7 day**
1:1	0.175 ± 0.0014	0.188 ± 0.0020	0.221 ± 0.0025	0.201 ± 0.0021
3:1	0.177 ± 0.0019	0.201 ± 0.0007	0.217 ± 0.0019	0.209 ± 0.0013
5:1	0.182 ± 0.0022	0.233 ± 0.0012	$0.256 \pm 0.0010*$	0.242 ± 0.0008
6:1	0.207 ± 0.0014	0.225 ± 0.0013	0.227 ± 0.0015	0.214 ± 0.0011

Linxin *et al. BMC Chemistry*　　　(2020) 14:57

Page 5 of 8

Fig. 9 In vitro release curve of Methadone loaded by $Zn_2(EBNB)_2(BPY)_2 \cdot 2H_2O$

was used as the drug group to study the cytotoxicity of $Zn_2(EBNB)_2(BPY)_2 \cdot 2H_2O$ on HeLa cells in vitro. The results of in vitro cytotoxicity experiments shows that the survival rate of HeLa cells decreased with the increase of $Zn_2(EBNB)_2(BPY)_2 \cdot 2H_2O$'s concentration after 36 h of exposure to different concentrations of $Zn_2(EBNB)_2(BPY)_2 \cdot 2H_2O$. When the concentration of $Zn_2(EBNB)_2(BPY)_2 \cdot 2H_2O$ was less than 20 μ g·ml^{-1}, the survival rate of HeLa cells was higher than that of the control group P > 0.05(Significant difference level). But when the concentration of $Zn_2(EBNB)_2(BPY)_2 \cdot 2H_2O$ is more than 20 μg·ml^{-1}, the cell survival rate decreases with the increase of $Zn_2(EBNB)_2(BPY)_2 \cdot 2H_2O$'s concentration. When the concentration of $Zn_2(EBNB)_2(BPY)_2 \cdot 2H_2O$ is 250 μg·ml^{-1}, the cell survival rate reaches the lowest value.

Conclusions

To sum up, $Zn_2(EBNB)_2(BPY)_2 \cdot 2H_2O$ can be synthesized by solvothermal method via (E)-bis(p-3-nitrobenzoic acid) ethylene ligand ($C_{16}H_{10}N_2O_8$). After drying and activation treatment, $Zn_2(EBNB)_2(BPY)_2 \cdot 2H_2O$ was loaded into Methadone with high drug loading. And the drug release curve shows that $Zn_2(EBNB)_2(BPY)_2 \cdot 2H_2O$ has slow-release function and can prolong Methadone's work. In addition, $Zn_2(EBNB)_2(BPY)_2 \cdot 2H_2O$ has good biocompatibility and is expected to become an excellent drug carrier.

In this study, MOFs was introduced into the field of drug release. Some features of MOFs, such as high specific surface area; tailorable, designable, adjustable channel size and channel surface functionalization, are used to study the sustained-release mechanism of MOFs as a new drug delivery form. All of these provide reference information for the research and development of new dosage forms of anti-drug addiction.

Experimental

Chemistry

Sources of experimental materials

Methadone used in this experiment was purchased from the purchasing point designated by the Ministry of public security of China, the Academy of criminal Sciences of Shanghai Public Security Bureau. All the other experimental materials used are commercially available.

Synthesis of (E)–bis (p-3-nitrobenzoic acid) ethylene ligand ($C_{16}H_{10}N_2O_8$)

200 ml concentrated sulfuric acid was pouring into a 400 ml flask, and 100 ml fuming nitric acid was added under 0 °C ice water bath while stirring constantly. Then 10 g of p-chloromethylbenzoic acid was added in small parts. After 90 min of reaction, p-chloromethylbenzoic acid was completely dissolved into the mixed acid. All substances in the bottle was pouring into 600 ml of ice water, a large amount of white solid is precipitated immediately. The residual mix-acid was filtered and washed, and then the product was recrystallized in toluene solvent. The white crystal of 3-nitro-p-chloromethylbenzoic acid was obtained and dried in an oven (Yield: 89%). ^{1}HNMR(200 MHz DMSO-d_6)δ8.76(s,1H);8.36(d,1H);7.87(d,1H);5.03(s,2H).

50 ml anhydrous ethanol was poured into a 300 ml beaker, and 5.7 g KOH was dissolved in it. Then 5.00 g of 3-nitro-p-chloromethylbenzoic acid was poured into form brown precipitate, which is potassium salt of (E)–di (p-3-nitrobenzoic acid) ethylene. After reaction at room temperature for 45 min, the solid was vacuumed and dissolved in 70 ml water. After that, adding HCl to the aqueous solution to adjust pH = 1 then form a precipitate. The solid was collected and recrystallized with tetrahydrofuran solvent. The yellow crystal compound (E)-di(p-3-nitrobenzoic acid) vinyl ($C_{16}H_{10}N_2O_8$) was obtained and dried in an oven (Yield: 78%). ^{1}HNMR(200 MHz DMSO-d_6)δ7.62(s,2H);7.89(d,2H);8.52(d,2H);9.06(s,2H).

Synthesis of $Zn_2(EBNB)_2(BPY)_2 \cdot 2H_2O$

The (E)-di(p-3-nitrobenzoic acid) ethylene ligand ($C_{16}H_{10}N_2O_8$) (0.15 mmol), 4,4′-bipyridine ligand (BPY,0.15 mmol), zinc nitrate ($Zn(NO_3)_2 \cdot 6H_2O$,0.15 mmol), ethanol 2 ml and H_2O 10 ml were put into a 50 ml high-pressure reactor, and the pH was adjusted to 9, ultrasounded, 150 °C for 2 days. The rhombic yellow crystal (E)-di(p-3-nitrobenzoic acid) ethylene can be obtained after filtration and washing. (Yield: 60%) Element analysis: C 52.45, n 9.34, H 3.11, Zn 10.89%; theoretical value: C 52.37, N 9.40, H 3.02, Zn 10.98%. The product is composed of $C_{26}H_{18}N_4O_9Zn$ (595.81).

Linxin *et al. BMC Chemistry*   (2020) 14:57

Page 6 of 8

Determination of structure

The suitable crystals of $Zn_2(EBNB)_2(BPY)_2 \cdot 2H_2O$ were selected for X-ray diffraction study. Diffraction data were collected on a Bruker SMART APEX-II CCD diffractometer equipped with a graphite-monochromated Mo-Kα radiation (λ = 0.71073 Å) by ρ-ω diffraction data at 298(2) K. All diffraction data through the SADABS software with multi-scan semi-empirical method of absorption correction. The structure were solved by direct methods and subsequent successive difference Fourier maps, and the structure was refined by full-matrix least-squares techniques on F^2 using SHELXL-2014 program [22]. The crystal structure refinement software was $Olex^2$(Version 1.2.7). The main crystallographic data are listed in the Tables 2, 3 and 4.

All hydrogen atoms were included in their calculated positions and treated as riding atoms with the U iso values assigned to 1.2U eq of their bonding carbon atoms and to 1.5U eq of their bonding oxygen atoms, respectively.

CCDC: 1545065 for 3-nitro-p-chloromethylbenzoic acid.

CCDC: 912099 for (E)-di(p-3-nitrobenzoic acid) vinyl.

CCDC: 910300 for $Zn_2(EBNB)_2(BPY)_2 \cdot 2H_2O$.

Table 2 Crystallographic data and structural correction conditions of 3-nitro-p-chloromethylbenzoic acid

Empirical formula	$C_7H_5ClN_2O_4$
Fomular weight	216.58
Crystalsystem	Monoclinic
Space group	P2(1)/c
Wavelength(Å)	0.71073
Temperature(K)	293(2)
a (Å)	7.5316(7)
b (Å)	17.0508(15)
c (Å)	14.1080(13)
α(°)	90.00
β(°)	100.6050(10)
γ(°)	90.00
V (Å³)	1780.8(3)
Z	8
Density (g/cm³)	1.515
μ(mm⁻¹)	0.418
F(000)	880
θ range (°)	2.389 to 23.956
GOF on F^2	1.036
R_1, wR_2 [I > 2σ(I)]	$R_1 = 0.0661$
	$wR_2 = 0.1719$
R_1, wR_2 (all data)	$R_1 = 0.1127$
	$wR_2 = 0.2159$

Table 3 Crystallographic data and structural correction conditions of (E)-di(p-3-nitrobenzoic acid) vinyl

Empirical formula	C16H13N2O9
Crystalsystem	Triclinic
Wavelength(Å)	0.71073
a(Å)	7.3757(4)
c(Å)	15.2903(10)
β(°)	82.9270(10)
V(Å3)	818.92(9)
Density (g/cm3)	1.545
F(000)	398
GOF on F2	1.029
Fomular weight	385.28
Space group	P-1
Temperature(K)	293(2)
b(Å)	7.7827(5)
α(°)	79.473(4)
γ(°)	72.069(4)
Z	2
μ(mm-1)	0.132
θ range (°)	2.717 to 28.347
R_1, wR_2 [I > 2σ(I)]	$R_1 = 0.0444$
	$wR_2 = 0.1161$
R_1, wR_2 (all data)	$R_1 = 0.0600$
	$wR_2 = 0.1321$

Table 4 Crystallographic data and structural correction conditions of $Zn_2(EBNB)_2(BPY)_2 \cdot 2H_2O$

Empirical formula	$C_{26}H_{18}N_4O_9Zn$
Fomular weight	595.81
Crystal system	Triclinic
Space group	P-1
Wavelength(Å)	0.71073
Temperature(K)	293(2)
a(Å)	8.1862(9)
b(Å)	11.4220(14)
c(Å)	14.2863(17)
α(°)	96.8030(10)
β(°)	93.0450(10)
γ(°)	102.472(2)
V(Å³)	1290.8(3)
Z	2
Density (g/cm³)	1.533
μ(mm⁻¹)	1.013
F(000)	608
θ range (°)	2.557 to 26.079
GOF on F^2	1.008
R_1, wR_2 [I > 2σ(I)]	$R_1 = 0.0499$
	$wR_2 = 0.1067$
R_1, wR_2 (all data)	$R_1 = 0.0750$
	$wR_2 = 0.1153$

Methadone loaded into Zn₂(EBNB)₂(BPY)₂·2H₂O

Accurately weigh proper amount of Methadone, and prepar the solution with methanol solvent. The maximum absorption peak is 292 nm. Then the concentration gradient of the standard solution was prepared, and the standard curves of absorbance (A) and concentration (c) at this wavelength were established. The standard curve is suitable for drug loading environment.

In the same way as the above operation, the appropriate concentration of Methadone solution was prepared with phosphate buffer (PBS, pH = 7.4) as the solvent, and the standard curves of absorbance (A) and concentration (c) were established with PBS as the blank control. The standard curve is suitable for drug releasing environment.

Accurately weigh 2 mg of dried and activated $Zn_2(EBNB)_2(BPY)_2 \cdot 2H_2O$, add in 1 ml of methanol solution which contain 10 mg of Methadone, mixing under ultrasound, acting for 24 h. Then centrifugate the reaction solution (10000 rpm, 10 min), take 100 μl of the supernatant and dilute it to 10 ml (100 times), measure its absorbance at 292 nm, then calculate the drug loading of $Zn_2(EBNB)_2(BPY)_2 \cdot 2H_2O$.

Drug loading

$$= \left(\text{Amount of drug in MOF/Total mass of MOF} \right) \times 100\%$$

In vitro release of methadone from Zn₂(EBNB)₂(BPY)₂·2H₂O

Take 2 mg of $Zn_2(EBNB)_2(BPY)_2 \cdot 2H_2O$ loaded with Methadone and put it into 20 ml PBS buffer solution, which is the experimental group. Take another 1.16 mg of $Zn_2(EBNB)_2(BPY)_2 \cdot 2H_2O$ and put it into 20 ml PBS buffer, which is the blank group. Under $(37 \pm 1 \text{ °C})$ constant temperature oscillator (oscillation speed: 100r·Min^{-1}), take 1 ml of solution every 12 h and add in equal amount of fresh PBS buffer, then centrifugate the solution (12000 rpm, 20 min), after that take the supernatant to determine its absorbance by ultraviolet spectrum. The content of Methadone in the solution was calculated according to the established Methadone standard curve, and the relationship curve between cumulative release and time was drawn. The in vitro releasing performance of Methadone from $Zn_2(EBNB)_2(BPY)_2 \cdot 2H_2O$ was investigated accordingly.

Cytotoxicity of Zn₂(EBNB)₂(BPY)₂·2H₂O

HeLa cells were cultured in RPMI 1640 medium, which contains 10% fetal bovine serum. HeLa cells were used only at logarithmic growth stage and good growth state. Cells were digested with 0.25% trypsin and centrifuged to precipitate. RPMI 1640 culture medium which contains 10% fetal bovine serum was used to prepare cell suspension with a cell density of 1×10^5 cells·ml^{-1}. Then it was inoculated into 96 well culture plate (104 cells per well, six multiple holes, each hole was 100 μ L.).

Then the culture plate was transferred to the incubator, and 100μ L RPMI 1640 culture medium was replaced at 37 °C, 5% CO_2 and saturated humidity for 24 h. The experiment was divided into three groups: blank control (without cells), negative control (without cells, without $Zn_2(EBNB)_2(BPY)_2 \cdot 2H_2O$), $Zn_2(EBNB)_2(BPY)_2 \cdot 2H_2O$ (with cells, with $Zn_2(EBNB)_2(BPY)_2 \cdot 2H_2O$). Then, 100μL solution of each group was added into make the mass concentration of 200, 100, 50, 25, 12, 6 μg·ml^{-1} respectively, then continue to culture for 48 h. Then change 100μL RPMI 1640 culture solution for each hole and 20μL MTT solution (5 mg·ML^{-1}) was added. Shake it on a micro oscillator for 20 min, continue to culture for 24 h. Remove the culture solution, added in 150μL DMSO for each hole, absorbance (A) at 490 nm was determined by enzyme-linked immunosorbent assay. The cell survival rate can be calculated by accordingly.

$$\text{Survival rate\%}$$
$$= \left(\text{Drug group - Blank group} \right)$$
$$/ \left(\text{Negative control group - Blank group} \right) \times 100\%.$$

Linxin *et al. BMC Chemistry* (2020) 14:57

Page 8 of 8

Author details
[1] Department of Drug Control, Key Laboratory of Narcotics Assay and Control Technology Ministry of Public Security, Yunnan Police College, Kunming 650223, China. [2] College of Science, Yunnan Agricultural University, Kunming 650201, China.

References
1. Mattick R P, Breen C, Kimber J, et al. Methadone maintenance therapy versus no opioid replacement therapy for opioid dependence[J]. Cochrane database of systematic reviews (Online), 2009, 3(3):CD002209
2. Crews J C, Sweeney N J, Denson D D. Clinical efficacy of methadone in patients refractory to other mu-opioid receptor agonist analgesics for management of terminal cancer pain. Case presentations and discussion of incomplete cross-tolerance among opioid agonist analgesics.[J]. Cancer, 2015, 72(7):2266-2272
3. Coppola M, Sacchetto G, Mondola R (2019) Craving for heroin: difference between methadone maintenance therapy patients with and without ADHD. Trends Psychiatry Psychother 41(1):83–86
4. Peng S, Jiang H, Du J, et al. Methadone Dosage and Plasma Levels, SNPs of OPRM1 Gene and Age of First Drug Use Were Associated With Outcomes of Methadone Maintenance Treatment. Frontiers in Genetics, 2018, 9
5. Ledgerwood DM, Lister JJ, Laliberte B et al (2019) Injection opioid use as a predictor of treatment outcomes among methadone-maintained opioid-dependent patients. Addict Behav 90:191–195
6. Jamie L. Miller, PharmD, BCPS, BCPPS, FPPAG, Kimberly Ernst, M F, Neely S B, et al. Low-dose versus high-dose methadone for the management of neonatal abstinence syndrome. Journal of opioid management, 2019, 15(2):159
7. Bao-Liang Z, Yan-Min X, Jun-Hong Z et al (2018) Non-suicidal self-injury in Chinese heroin-dependent patients receiving methadone maintenance treatment: prevalence and associated factors. Drug Alcohol Depend 189:161–165
8. Gómez-López L, Sala-Blanch X, Gambús Cerrillo PL et al (2018) Outpatient intravenous multimodal elastomeric pump with methadone in ambulatory surgery. Revista Espaola De Anestesiología Y Reanimación 65(6):306–313
9. Dao ATM, Nguyen HTT, Nguyen LH (2018) Variation Overtime among Patients of the Six Methadone Maintenance Treatment Clinics in Thai Nguyen from 2011 to 2015. Biomed Res Int 2018:1–7
10. Premkumar A, Grobman W A, Terplan M, et al. 740: Methadone, buprenorphine, or detoxification for management of perinatal opioid use disorder: a cost-effectiveness analysis. American Journal of Obstetrics and Gynecology, 2019, 220(1)
11. Zhang R, Zhou T, Wang L et al (2018) Metal-organic frameworks-derived hierarchical Co3O4 structures as efficient sensing materials for acetone detection. ACS Appl Mater Interfaces 10(11):9765
12. Guillerm V, Kim D, Eubank JF et al (2014) A supermolecular building approach for the design and construction of metal–organic frameworks. Chem Soc Rev 43(16):6141–6172
13. Sule R, Mishra AK (2020) MOFs-carbon hybrid nanocomposites in environmental protection applications. Environ Sci Pollut Res 27(14):16004–16018
14. Karmakar A, Desai A V, Ghosh S K. Ionic metal-organic frameworks (iMOFs): Design principles and applications. Coordination Chemistry Reviews, 2016, 307(JAN.PT.2):313-341
15. Spokoyny AM, Farha OK, Mulfort KL et al (2010) Porosity tuning of carborane-based metal–organic frameworks (MOFs) via coordination chemistry and ligand design. Inorg Chim Acta 364(1):266–271
16. Banerjee R (2012) Porous metal organic frameworks (MOFs) for reversible gas storage and sequestration applications. J Indian Chem Soc 89(9):1197–1202
17. Tan LL, Li H, Zhou Y et al (2015) Zn2＋-triggered drug release from biocompatible zirconium MOFs equipped with supramolecular gates. Small 11(31):3807–3813
18. Gao Rui-Cheng, Guo Fu-Sheng, Bai Nan-Nan et al (2016) Two 3D isostructural Ln(III)-MOFs: displaying the slow magnetic relaxation and luminescence properties in detection of nitrobenzene and Cr2O7(2). Inorg Chem 55(21):11323
19. Publishing R (2013) Towards acid MOFs–catalytic performance of sulfonic acid functionalized architectures. Catal Sci Technol 3(9):2311–2318
20. Jacobsen J, Achenbach B, Reinsch H et al (2019) The first water-based synthesis of Ce(IV)-MOFs with saturated chiral and achiral C4-dicarboxylate linkers. Dalton Trans 48(23):8433–8441
21. Song LI, Lin-Xin DENG, Jun-Jie HE et al (2014) Synthesis and Characterization of Two Metal-Organic Frameworks(MOFs) with Nitro Group Functionalization Ligands. Chinese J Inorganic Chem 30(10):2401–2407
22. Sheldrick GM (2007) A short history of SHELX. Foundations of Crystallography, Acta Crystallographica Section A, p 64

Publisher's Note
Springer Nature remains neutral with regard to jurisdictional claims in published maps and institutional affiliations.